

Spin-orbit-enhanced Wigner localization in quantum dots

A. Cavalli¹, F. Malet², J. C. Cremon², and S. M. Reimann²

¹*DTU Nanotech, DTU, DK-2800 Kgs. Lyngby, Denmark*

²*Mathematical Physics, Lund University, LTH, P.O. Box 118, SE-22100 Lund, Sweden*

(Dated: September 24, 2018)

We investigate quantum dots with Rashba spin-orbit coupling in the strongly-correlated regime. We show that the presence of the Rashba interaction enhances the Wigner localization in these systems, making it achievable for higher densities than those at which it is observed in Rashba-free quantum dots. Recurring shapes in the pair distribution functions of the yrast spectrum, which might be associated with rotational and vibrational modes, are also reported.

PACS numbers: 73.21.-b, 73.21.La, 73.63.Kv

I. INTRODUCTION

Electron localization in finite-size nanostructures, reminiscent of the Wigner crystallization of the bulk electron gas¹, occurs when the density of the system becomes low enough so that the Coulomb repulsion dominates over the motion associated with the kinetic energy of the electrons. As a consequence, the electrons “crystallize”, acting as classical charges seeking for the equilibrium positions that minimize their total energy. From the theoretical point of view, this phenomenon has been extensively investigated in e.g. quantum dots (QDs)^{2–5} (see also the review Ref. 6), quantum wires⁷, and quantum rings⁸, and analogue Wigner-localized states have also been observed in other quantum systems such as e.g. ultracold atomic gases, ultracold trapped ions, complex plasmas, or cuprate chain compounds⁹. On the experimental side, signatures of electron localization have been found in e.g. quantum dots¹⁰, quantum wires¹¹, or carbon nanotubes¹². The study of this phenomenon is not only interesting from the purely fundamental point of view, but it has also been shown that Wigner-localized systems can be useful to design e.g. chains of spatially separated quantum bits¹² or quantum hard drives¹³.

In experiments with semiconductor quantum dots and wires, however, difficulties are encountered when lowering the density down to the regimes at which Wigner localization is achieved due to disorder effects^{10,11}. The search for more clear and direct experimental evidence of Wigner localization in such systems, as well as for ways that allow its observation at more easily accessible densities, is therefore an interesting matter of research.

In the context of semiconductor nanostructures, the study of the effects of the so-called Dresselhaus¹⁴ (DSOI) and Rashba¹⁵ spin-orbit interactions (RSOI) has also attracted great interest in the last years. The origin of these interactions is due to the existence of internal asymmetries that give rise to net electric fields within the heterostructures. In the reference frame of the electrons, these electric fields transform into effective magnetic fields, which couple to the electronic spins. In the case of the Rashba spin-orbit coupling, which is due to the asymmetry of the potential well confining the conduction electrons within the heterostructure, special at-

tention has been paid since it was shown that its strength can be experimentally tuned within large ranges of values by means of the application of external electric fields¹⁶ or by changing the electron density¹⁷, making of this mechanism a very promising tool for potential applications in e.g. spintronics or quantum computation since it provides a natural way to control and manipulate the electronic spin¹⁸.

Important effects due to the spin-orbit (SO) interaction in semiconductor nanostructures have been reported on, e.g., the addition energies, the electron g-factor, the magnetoconductivity, the spin textures, or the spin-relaxation properties¹⁹. Also, spin-orbit-induced electron localization has been observed in Coulomb-free closed loops of quantum wires with Rashba SO coupling, as well as in quantum rings with both RSOI and DSOI²⁰. It must be pointed out, however, that this localization is not of the Wigner-type since the electrons are considered to be non-interacting, but is entirely due to the analogies and the interplay of the spin-orbit coupling with external magnetic fields, which gives rise to Aharonov-Bohm cages and periodic trapping potentials that cause the localization of the particles²⁰. As a matter of fact, the electron-electron interaction has been taken into account in a rather small fraction of the many studies on the spin-orbit coupling in semiconductor nanostructures, and only a few have treated it without approximations or have considered its interplay with the SO terms²¹.

In this Letter, we investigate strongly-correlated InAs quantum dots with RSOI and we show that Wigner localization is largely enhanced by the presence of the Rashba coupling, making this phenomenon potentially observable at sensibly higher electronic densities than those at which it is achieved in spin-orbit-free QDs. Since the Dresselhaus contribution is expected to be small in narrow-bandgap materials such as InAs²², we neglect it in the present study.

II. MODEL AND METHOD

We consider a two-dimensional InAs quantum dot with parabolic confinement in the xy -plane given by $V(\mathbf{r}) = (1/2)\omega^2(x^2 + y^2)$. The Rashba spin-orbit coupling is de-

scribed by the usual term¹⁵

$$H_R = \frac{\hbar k_R}{m^* m_e} [p_y \sigma_x - p_x \sigma_y], \quad (1)$$

where $m^* m_e$ is the electron effective mass, with $m^* = 0.023$, p_i is its linear momentum in the i -direction, σ_i is the corresponding Pauli matrix, and k_R determines the strength of the interaction.

The QD is considered to have N electrons interacting with each other through the Coulomb interaction. Expressing the energies and lengths in units of $\hbar\omega$ and $l_\omega = \sqrt{\frac{\hbar}{m^* m_e \omega}}$ respectively, the full Hamiltonian of the system, in second quantization form, reads

$$\begin{aligned} H = & \sum_{\alpha\beta} \langle \alpha | \frac{p_x^2}{2} + \frac{p_y^2}{2} + \frac{1}{2} (x^2 + y^2) \\ & + \widetilde{k}_R [p_y \sigma_x - p_x \sigma_y] | \beta \rangle a_\alpha^\dagger a_\beta \\ & + \frac{1}{2} \sum_{\alpha\beta\gamma\delta} \langle \alpha, \beta | \frac{g}{|\mathbf{r} - \mathbf{r}'|} | \gamma, \delta \rangle a_\alpha^\dagger a_\beta^\dagger a_\gamma a_\delta, \quad (2) \end{aligned}$$

where a_μ^\dagger , a_μ ($\mu = \alpha, \beta, \gamma, \delta$) are the usual creation and annihilation operators for the single-particle state $|\mu\rangle$, and $\widetilde{k}_R \equiv l_\omega k_R$ is a dimensionless parameter determining the effective spin-orbit interaction strength. The prefactor in the Coulomb term is given by $g = e^2 / (4\pi\epsilon_0\epsilon_r l_\omega \hbar\omega) = l_\omega / a_B^*$, where a_B^* is the effective Bohr radius, which for InAs is approximately 34 nm. The confinement frequency is related to the average electron density n through the relation $\omega^2 = \hbar^2 / (m^2 a_B^* \sqrt{N} r_s^3)$,³ where $r_s = 1/\sqrt{\pi n}$ is the Wigner-Seitz radius.

Using the configuration-interaction method, we numerically find the many-particle eigenstates of the system, expanded in a basis of Slater determinants made up of 2D harmonic-oscillator single-particle orbitals $|\mu\rangle = |n, m, s\rangle$, where n , m and $s = \uparrow, \downarrow$ are, respectively, the radial, azimuthal, and spin quantum numbers. Defining the equivalent set $n_\pm \equiv (2n + |m| \pm m)/2$, one has for the matrix elements of the Rashba term:

$$\begin{aligned} \langle n', m', \uparrow | H_R | n, m, \uparrow \rangle = \langle n', m', \downarrow | H_R | n, m, \downarrow \rangle = 0, \\ \langle n_+, n_-, \uparrow | H_R | n_+, n_-, \downarrow \rangle = -\widetilde{k}_R \times \\ [\sqrt{n_- + 1} \delta_{n_+, n_+'} \delta_{(n_+ + 1), n_+'} - \sqrt{n_+} \delta_{(n_+ - 1), n_+'} \delta_{n_-, n_+'}], \\ \langle n_+, n_-, \downarrow | H_R | n_+, n_-, \uparrow \rangle = \widetilde{k}_R \times \\ [\sqrt{n_+ + 1} \delta_{(n_+ + 1), n_+'} \delta_{n_-, n_+'} - \sqrt{n_-} \delta_{n_+, n_+'} \delta_{(n_- - 1), n_+'}] \quad (3) \end{aligned}$$

The (in principle) infinitely large basis space is truncated, taken to be large enough to ensure converged solutions, which in our calculations are achieved with 15 harmonic oscillator shells. As the total angular momentum $J_z = L_z + S_z$ represents a good quantum number, the diagonalization is in practice done separately for each considered J_z .

A standard value for the confinement energy is of the order of $\hbar\omega \sim 5$ meV, with associated effective Coulomb

strength $g = 0.75 \equiv g_0$. We have studied the interval $g_0 \leq g \leq 3g_0$, corresponding to $5 \text{ meV} \leq \hbar\omega \leq 0.56 \text{ meV}$. Finally, regarding the RSOI term, we have considered the range $0.263 \leq \widetilde{k}_R \leq 2.63$, and we have found that the spin-orbit-induced localization effects become clearly observable for strengths of the Rashba coupling constant $\hbar^2 k_R / m \gtrsim 8.5 \times 10^{-11} \text{ eV}\cdot\text{m}$. While being slightly more than two times larger than the ones experimentally accessible nowadays^{17,23}, such values should be reachable in the near future considering the ongoing research on new materials with larger SO couplings²⁴.

III. RESULTS

When the RSOI is neglected ($k_R = 0$), we find that the electrons start to localize only for strengths of the Coulomb interaction larger than $\sim 5g_0$, corresponding to $r_s \gtrsim 4.4a_B^*$, as expected^{3,4}. For weaker interactions, we only observe a slight deformation of the electron cloud as a whole. Also, when the localization occurs, there is a depletion of the electron density in the center of the trap due to the repulsion between the particles.

This scenario, however, sensibly changes when the Rashba term is taken into account. In Figs. 1 and 2 we show the pair distribution function

$$PDF(\mathbf{r}, \mathbf{r}') = \langle \hat{\psi}^\dagger(\mathbf{r}) \hat{\psi}^\dagger(\mathbf{r}') \hat{\psi}(\mathbf{r}') \hat{\psi}(\mathbf{r}) \rangle, \quad (4)$$

which gives the probability of finding a particle at the position \mathbf{r} provided that another one is at \mathbf{r}' , for the 3- and 4-electron quantum dots for different strengths of the effective spin-orbit and Coulomb interactions. One can clearly see that the inclusion of the Rashba term, and especially for large values of \widetilde{k}_R , significantly enhances the electron localization. Indeed, in both cases it is already visible for $\widetilde{k}_R = 1.84$ and $g = 3g_0$, corresponding to $\hbar\omega = 0.56 \text{ meV}$ and $\hbar^2 k_R / m = 8.5 \times 10^{-11} \text{ eV}\cdot\text{m}$, with the electrons distributing themselves on the vertices of an equilateral triangle and of a square, respectively, analogously to what is observed in quantum dots submitted to perpendicular magnetic fields^{2,10}. This corresponds to Wigner-Seitz radii of $r_s = 2.5a_B^*$ for $N = 3$ and to $r_s = 2.4a_B^*$ for $N = 4$, i.e. almost half the values at which localization is observed in spin-orbit-free quantum dots. A further increase of the RSOI while keeping the confinement strength fixed leads to a more pronounced localization of the electrons, as can be seen from the figures when $\widetilde{k}_R = 2.63$.

We have also investigated a dot with six electrons, although in this case an optimal convergence of the numerical simulations has not been possible to achieve. Nevertheless, we have observed that the behavior of the system is qualitatively similar to the cases with $N = 3$ and $N = 4$, with localized configurations appearing at similar effective Coulomb strengths with $r_s \sim 2.2a_B^*$, made up of five electrons forming a pentagon with the sixth one placed at the center of the dot. Finally, we also

want to mention that in some papers electron localization has been addressed making use of quantitative suitable criteria^{5,25}. In our study, however, we have limited ourselves to the rather qualitative discussion presented above.

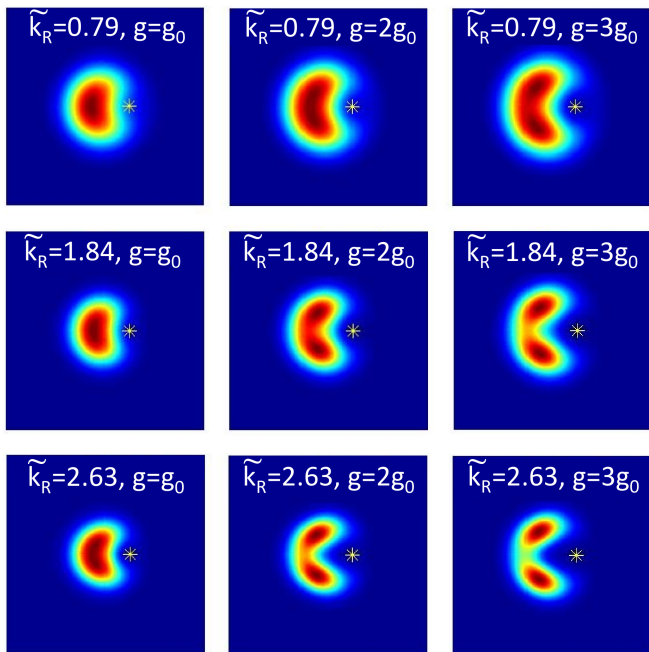


FIG. 1: Pair distribution functions for the 3-electron quantum dot and for different strengths of the effective Rashba (increasing from top to bottom) and Coulomb (increasing from left to right) interactions. The star symbol indicates the position of the reference electron.

The enhancement of the Wigner localization due to the Rashba spin-orbit coupling can be qualitatively explained already from the non-interacting-electron picture. Indeed, we have observed that the spatial extension of the single-particle density profiles is reduced when the RSOI term is taken into account as compared to the harmonic oscillator case with $k_R = 0$. This is in close analogy with the Fock-Darwin single-particle states of quantum dots under magnetic fields²⁶ and may be understood from the nature of the spin-orbit interaction described above. Therefore, it can be concluded that one of the effects of the Rashba coupling is to minimize the overlapping between the different electrons and thus to favour their spatial separation with respect to each other.

It is also interesting to study the so-called yrast spectrum²⁷, i.e., the lowest energy level for a given total angular momentum, which we plot in Fig. 3 for the three-electron dot in different parameter regimes. This again shows very close analogy with what is observed in quantum dots under perpendicular magnetic fields², the main difference being in the low J_z range. In the Rashba case, low $|j_z|$ single-particle states are almost degenerate and therefore the spectrum is rather flat for low values of J_z . On the contrary, under an applied magnetic field,

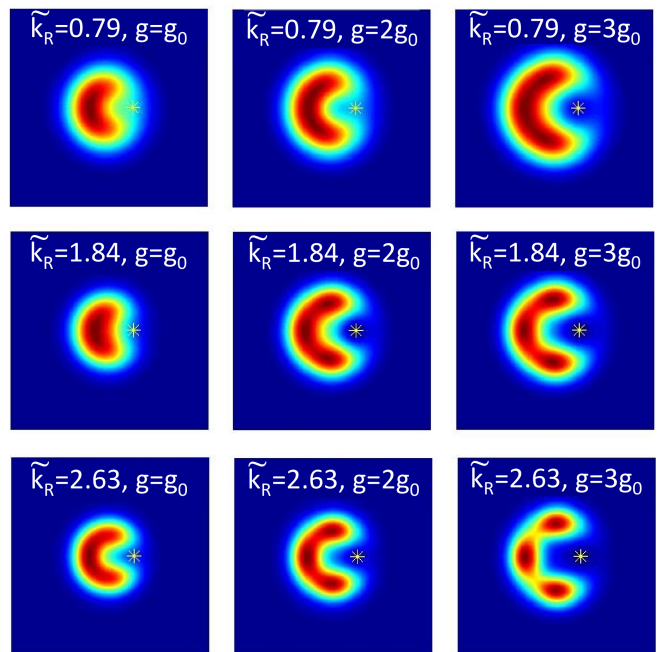


FIG. 2: Same as Fig. 1 for the quantum dot with $N = 4$.

a preferred spin direction is selected and low J_z states, realized using s.p. states of opposite angular momentum, are energetically unfavourable. This explains the overall parabolic shape of the yrast profiles shown in², different from the almost degenerate low J_z levels in the Rashba case. For higher angular momenta, however, the magnetic and Rashba yrast spectra become more similar: in both cases the yrast lines show oscillations with period N , which become more pronounced as the Coulomb repulsion increases. The presence of these oscillations is explained in Ref. 2 by the vanishing of the exchange energy term for configuration with electrons occupying adjacent j_z single-particle levels, which occur only for every third unit of angular momentum. Moreover, for the strong magnetic field case –and thus for high J_z – it can be seen that the electrons behave as a rigid, molecule-like configuration^{2,28}. A semiclassical interpretation of the yrast spectrum is then possible, with the local minima corresponding to purely rotational modes and with the intermediate states containing at least one vibrational quantum²⁹.

Finally, a qualitative signature of the above-mentioned molecular behaviour in the Rashba-interacting case can be observed from Fig. 4, where we show the pair distribution functions corresponding to the Wigner-localized case for different values of the total angular momentum. One can recognize recurring shapes ($J_z = 7.5\hbar$ and $J_z = 10.5\hbar$, $J_z = 8.5\hbar$ and $J_z = 11.5\hbar$, $J_z = 9.5\hbar$ and $J_z = 12.5$), which might be associated with specific rotational and vibrational states for localized electrons in quantum dots. Indeed, the standard triangular shapes are found at the local minima, consistently with the hypothesis that they correspond to rotational modes, where

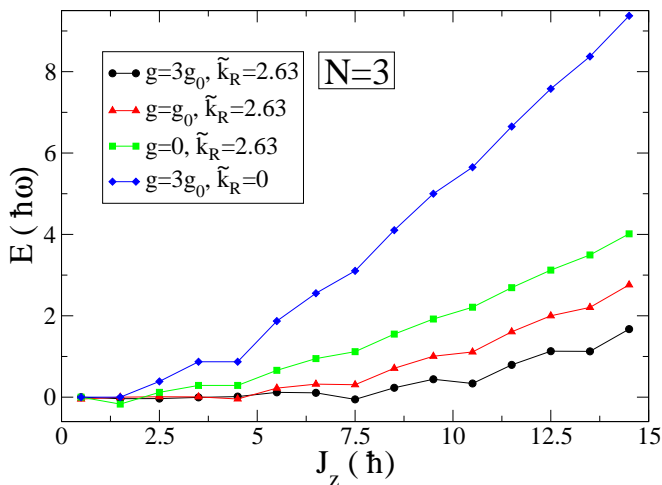


FIG. 3: Yrast spectrum for the 3-electron quantum dot with $g = 3g_0$ and $\tilde{k}_R = 0$ (blue diamonds), $g = 0$ and $\tilde{k}_R = 2.63$ (green squares), $g = g_0$ and $\tilde{k}_R = 2.63$ (red triangles), and $g = 3g_0$ and $\tilde{k}_R = 2.63$ (black circles). The energies have been shifted to have the same value at $J_z = 0.5\hbar$ for a better comparison.

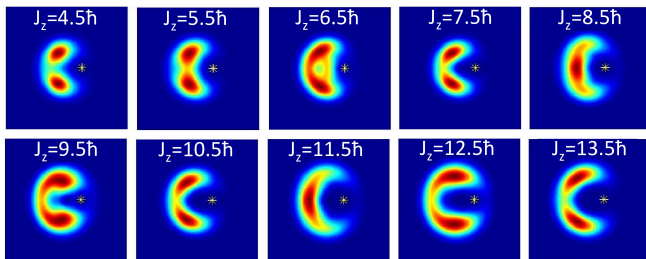


FIG. 4: Pair distribution functions for different values of J_z for the three-electron dot in the Wigner-localized regime ($g = 3g_0$ and $\tilde{k}_R = 2.63$).

no deformation is involved. Other shapes also appear pe-

riodically, and they look consistent with the vibrations of a triangular molecule (stretching and shrinking the triangle basis, for example, similarly as patterns previously observed²⁸). We think that the appearance of these deformed pair distribution functions matching the periodicity of the yrast spectrum is a strong hint of a “rigid-molecule” behavior of the electrons.

IV. CONCLUSIONS

In conclusion, we have found that the presence of Rashba spin-orbit coupling in strongly-correlated quantum dots largely enhances the Wigner localization in these systems and makes it observable at higher densities than in the spin-orbit-free case. We report several analogies with quantum dots under magnetic fields, and in particular we show that the pair distribution functions corresponding to the states of the yrast spectrum of the Wigner-localized dot present recurring shapes that one can associate with rotational and vibrational modes. Our results thus point out the importance of the experimental investigation of Wigner localization in materials with large spin-orbit coupling. Although not modeled here, any disorder in the material can be expected to contribute to further enhance the localization^{10,11}. The effects of the Dresselhaus spin-orbit interaction on the electron localization, and in particular its interplay with the Rashba term, is also an interesting subject that will be investigated in future works.

V. ACKNOWLEDGMENTS

We thank M. Koskinen, H. Linke, M. Manninen, and H.Q. Xu for discussions and valuable comments. This work was financed by the Swedish Research Council. We also thank the nmC@LU for support.

¹ E. P. Wigner, Phys. Rev. **46**, 1002 (1934).
² P. A. Maksym, Phys. Rev. B **53**, 10871 (1996).
³ S. M. Reimann, M. Koskinen, and M. Manninen, Phys. Rev. B **62**, 8108 (2000).
⁴ R. Egger, W. Häusler, C. H. Mak, and H. Grabert, Phys. Rev. Lett. **82**, 3320 (1999).
⁵ A. V. Filinov, M. Bonitz, and Yu. E. Lozovik, Phys. Rev. Lett. **86**, 3851 (2001).
⁶ S. M. Reimann and M. Manninen, Rev. Mod. Phys. **74**, 1283 (2002).
⁷ B. Tanatar, I. Al-Hayek, and M. Tomak, Phys. Rev. B **58**, 9886 (1998); Erich J. Mueller, Phys. Rev. B **72**, 075322 (2005); D. Hughes and P. Ballone, Phys. Rev. B **77**, 245312 (2008); A. D. Güçlü, C. J. Umrigar, Hong Jiang, and Harold U. Baranger, Phys. Rev. B **80**, 201302(R) (2009).
⁸ F. Pederiva, A. Emperador, and E. Lipparini, Phys. Rev.

B **66**, 165314 (2002); Leonardo Colletti, Francesc Malet, Marti Pi, and Francesco Pederiva, Phys. Rev. B **79**, 125315 (2009); J. M. Escartín, Francesc Malet, Agustí Emperador, and Mart Pi, Phys. Rev. B **79**, 245317 (2009).
⁹ Constantine Yannouleas and Uzi Landman, Rep. Prog. Phys. **70**, 2067 (2007); Jonas C. Cremon, G. M. Bruun, and S. M. Reimann, Phys. Rev. Lett. **105**, 255301 (2010); W. M. Itano, J. J. Bollinger, J. N. Tan, B. Jelenković, X.-P. Huang and D. J. Wineland, Science **279**, 686 (1998); M. Bonitz, C. Henning, and D. Block, Rep. Prog. Phys. **73** (2010) 066501; P. Horsch, M. Sofin, M. Mayr, and M. Jansen, Phys. Rev. Lett. **94**, 076403 (2005).
¹⁰ Sokratis Kalliakos, Massimo Rontani, Vittorio Pellegrini, César Pascual García, Aron Pinczuk, Guido Goldoni, Elisa Molinari, Loren N. Pfeiffer, and Ken W. West, Nature Physics **4**, 467 (2008).

- ¹¹ O. M. Auslaender, H. Steinberg, A. Yacoby, Y. Tserkovnyak, B. I. Halperin, K. W. Baldwin, L. N. Pfeiffer, and K. W. West, *Science* **308**, 88 (2005); L. H. Kristinsdóttir, J. C. Cremon, H. A. Nilsson, H. Q. Xu, L. Samuelson, H. Linke, A. Wacker, S. M. Reimann, *Phys. Rev. B* **83**, 041101 (2011).
- ¹² V. V. Deshpande and M. Bockrath, *Nature Physics* **4**, 314 (2008);
- ¹³ J. M. Taylor and T. Calarco, *Phys. Rev. A* **78**, 062331 (2008).
- ¹⁴ G. Dresselhaus, *Phys. Rev.* **100**, 580 (1955).
- ¹⁵ Yu. A. Bychkov and E. I. Rashba, *Sov. Phys.-JETP Lett.* **39**, 78 (1984).
- ¹⁶ J. Nitta, Tatsushi Akazaki, and Hideaki Takayanagi, Takatomo Enoki, *Phys. Rev. Lett.* **78**, 1335 (1997).
- ¹⁷ T. Matsuyama, R. Küirsten, C. Meißner, and U. Merkt, *Phys. Rev. B* **61**, 15588 (2000).
- ¹⁸ S. A. Wolf, D. D. Awschalom, R. A. Buhrman, J. M. Daughton, S. von Molnár, M. L. Roukes, A. Y. Chtchelkanova, and D. M. Treger, *Science* **294**, 1488 (2001); I. Žutić, Jaroslav Fabian, and S. Das Sarma, *Rev. Mod. Phys.* **76**, 323 (2004); Lorenz Meier, Gian Salis, Ivan Shorubalko, Emilio Gini, Silke Schön, and Klaus Ensslin, *Nature Physics* **3**, 650 (2007).
- ¹⁹ M. Governale, *Phys. Rev. Lett.* **89**, 206802 (2002); Stephan Weiss and R. Egger, *Phys. Rev. B* **72**, 245301 (2005); A. Ambrosetti, F. Pederiva, and E. Lipparini, *Phys. Rev. B* **83**, 155301 (2011); C. F. Destefani and Sergio E. Ulloa, *Phys. Rev. B* **71**, 161303(R)(2005); E. Lipparini, M. Baranco, F. Malet, and M. Pi, *Phys. Rev. B* **79**, 115310 (2009); M. M. Glazov and E. Ya. Sherman, *Phys. Rev. B* **71**, 241312 (2005); Denis V. Bulaev and Daniel Loss, *Phys. Rev. B* **71**, 205324 (2005).
- ²⁰ Dario Bercioux, Michele Governale, Vittorio Cataudella, and Vincenzo Marigliano Ramaglia, *Phys. Rev. Lett.* **93**, 056802 (2004); J. S. Sheng and Kai Chang, *Phys. Rev. B* **74**, 235315 (2006).
- ²¹ Tapash Chakraborty, and Pekka Pietiläinen, *Phys. Rev. B* **71**, 113305 (2005); P. Pietiläinen and T. Chakraborty, *Phys. Rev. B* **73**, 155315 (2006); Csaba Daday, Andrei Manolescu, D. C. Marinescu, Vidar Gudmundsson, arXiv:1106.3697v1 (2011); Stefano Chesi and Gabriele F. Giuliani, *Phys. Rev. B* **75**, 155305 (2007); Guang-Hong Chen and M. E. Raikh, *Phys. Rev. B* **60**, 4826 (1999).
- ²² G. Lommer, F. Malcher, and U. Rossler, *Phys. Rev. Lett.* **60**, 728 (1988).
- ²³ Y. Sato, T. Kita, S. Gozu, S. Yamada, *Journal of Applied Physics* **89**, 8017 (2001).
- ²⁴ Xiao-Jie Hao, Tao Tu, Gang Cao, Cheng Zhou, Hai-Ou Li, Guang-Can Guo, Wayne Y. Fung, Zhongqing Ji, Guo-Ping Guo and Wei Lu *Nano Lett.* **10**, 2956 (2010); L. E. De Long, L. Shlyk, G. Cao, R. Niewa, *Electromagnetics in Advanced Applications (ICEAA), 2010 International Conference on*, pp.591-594 (2010). doi: 10.1109/ICEAA.2010.5652217.
- ²⁵ J. Böning, A. Filinov, P. Ludwig, H. Baumgartner, M. Bonitz, and Yu. E. Lozovik, *Phys. Rev. Lett* **100**, 113401 (2008).
- ²⁶ P. A. Maksym and Tapash Chakraborty, *Phys. Rev. Lett.* **65**, 108 (1990).
- ²⁷ This concept was adopted from nuclear physics (see, e.g., A. Bohr and B. R. Mottelson, *Nuclear structure*, Benjamin, New York (1975)), and has been extensively used in quantum dot theory⁶, as well as in the study of vortex properties of quantum gases (see, e.g., H. Saarikoski, S. M. Reimann, A. Harju, and M. Manninen, *Rev. Mod. Phys.* **82**, 2785 (2010)).
- ²⁸ J.-P. Nikkarila and M. Manninen, *Phys. Rev. A* **76**, 013622 (2007); J. P. Nikkarila and M. Manninen, *Solid State Comm.* **141**, 209 (2007).
- ²⁹ M. Koskinen, M. Manninen, B. Mottelson, and S. M. Reimann, *Phys. Rev. B* **63**, 205323 (2001).